BIOLOGY OF REPRODUCTION (2015) **92**(5):121, 1–11
Published online before print 8 April 2015.
DOI 10.1095/biolreprod.114.127266

Flow Cytometry Analysis Reveals That Only a Subpopulation of Mouse Sperm Undergoes Hyperpolarization During Capacitation[1]

Jessica Escoffier,[4] Felipe Navarrete,[4] Doug Haddad,[4] Celia M. Santi,[5] Alberto Darszon,[3,6] and Pablo E. Visconti[2,4]

[4]*Department of Veterinary and Animal Science, Integrated Sciences Building, University of Massachusetts, Amherst, Massachusetts*
[5]*Department of Anatomy and Neurobiology. Washington University School of Medicine, St. Louis, Missouri*
[6]*Departamento de Genética del Desarrollo y Fisiología Molecular, Instituto de Biotecnologia-Universidad Nacional Autónoma de México, Cuernavaca, México*

ABSTRACT

To gain fertilizing capacity, mammalian sperm should reside in the female tract for a period of time. The physiological changes that render the sperm able to fertilize are known as capacitation. Capacitation is associated with an increase in intracellular pH, an increase in intracellular calcium, and phosphorylation of different proteins. This process is also accompanied by the hyperpolarization of the sperm plasma membrane potential (Em). In the present work, we used flow cytometry to analyze changes in sperm Em during capacitation in individual cells. Our results indicate that a subpopulation of hyperpolarized mouse sperm can be clearly distinguished by sperm flow cytometry analysis. Using sperm bearing green fluorescent protein in their acrosomes, we found that this hyperpolarized subpopulation is composed of sperm with intact acrosomes. In addition, we show that the capacitation-associated hyperpolarization is blocked by high extracellular K^+, by PKA inhibitors, and by SLO3 inhibitors in CD1 mouse sperm, and undetectable in *Slo3* knockout mouse sperm. On the other hand, in sperm incubated in conditions that do not support capacitation, sperm membrane hyperpolarization can be induced by amiloride, high extracellular $NaHCO_3$, and cAMP agonists. Altogether, our observations are consistent with a model in which sperm Em hyperpolarization is downstream of a cAMP-dependent pathway and is mediated by the activation of SLO3 K^+ channels.

capacitation, ENac, flow cytometry, membrane potential, SLO3

INTRODUCTION

After ejaculation, sperm have not yet acquired full fertilizing capacity. They need to undergo a maturational process in the female reproductive tract known as capacitation [1]. In mouse sperm, capacitation depends on fast activation of cAMP-dependent pathways, lipid remodeling of the plasma membrane [2–4], increases in intracellular pH (pH_i) [5, 6] and intracellular Ca^{2+} concentration ($[Ca^{2+}]_i$), and an increase in protein tyrosine phosphorylation [7–10]. At the functional level, capacitation induces changes in the motility pattern (e.g., hyperactivation) [1] and prepares the sperm to undergo a physiologically stimulated acrosome reaction (AR) [11–13]. Altogether, these changes render the sperm able to fertilize the egg.

It has been shown that capacitation in mouse sperm is also accompanied by hyperpolarization of the sperm plasma membrane potential (Em) [14]. The resting Em of non-capacitated mouse sperm lies between −35 and −45 mV and, after capacitation, this value reaches approximately −65 mV [15–23]. It has been hypothesized that this hyperpolarization is required to remove inactivation from T-type voltage-dependent Ca^{2+} channels (CaV3), which could then be activated during the AR by physiological agonists (e.g., ZP) [14, 24–26]. Although CaV3 channels can be detected by patch clamp in testicular sperm [27], their activity is lost in epididymal sperm [28], raising questions about the presence of this type of Ca^{2+} channel in mature sperm. Considering these data, the exact role of sperm hyperpolarization is not completely clear. However, our group has recently shown that, at least in mouse sperm, sperm membrane hyperpolarization is necessary and sufficient for an agonist-induced AR [15].

The molecular mechanisms involved in sperm hyperpolarization are not well established. Among the most likely possibilities, changes towards a more negative Em during sperm capacitation can be explained by: 1) the opening of K^+ channels, such as SLO3 [21, 29, 30] or other inward rectifiers [20, 31] or 2) the closing of Na^+ channels, such as the amiloride-sensitive epithelial Na^+ channels (ENaCs; [18, 32]) mediated by activation of the cystic fibrosis transmembrane regulator (CFTR; [32–35]). Favoring the first hypothesis is the observation that sperm from *Slo3*-null mice do not undergo the capacitation-associated hyperpolarization [31, 33, 36, 37]. In support of the second explanation, it has been established that permeability to Na^+ contributes to the sperm resting Em and that addition of amiloride is sufficient to hyperpolarize the sperm membrane in conditions that do not support capacitation. In a recent article, Santi's group evaluated both hypotheses using wild-type and *Slo3*-null sperm, and showed that, although inhibition of Na^+ channels does induce hyperpolarization, closing of Na^+ channels may not be the main mechanism by which the sperm membrane is hyperpolarized during capacitation [29]. The authors concluded that the most

[1]This study was supported by Eunice Kennedy Shriver National Institute of Child Health and Human Development grants National Institutes of Health [NIH] RO1 HD38082 and HD44044 to P.E.V., and NIH RO1 HD069631 to C.M.S., the Dirección General de Asuntos del Personal Académico/Universidad Nacional Autónoma de México grant DGAPA-UNAM IN225406-3, Consejo Nacional de Ciencia y Tecnologia grant 39908-Q, and Secretaría de Ciencia, Tecnología e Innovación del Distrito Federal, México grant 039/2013 to A.D.
[2]Correspondence: E-mail: pvisconti@vasci.umass.edu
[3]Correspondence: E-mail: darszon@ibt.unam.mx

Received: 3 December 2014.
First decision: 5 January 2015.
Accepted: 16 March 2015.

eISSN: 1529-7268 http://www.biolreprod.org
ISSN: 0006-3363

likely molecular mechanism responsible for membrane hyperpolarization in sperm is the activation of SLO3 K^+ channels.

Observations by multiple laboratories indicate that the sperm population is heterogeneous, and that only a fraction undergoes capacitation [32, 37]. However, most of what is known about the molecular basis of sperm capacitation derives from experiments using whole sperm populations. These suspensions contain sperm at different capacitation stages and also subpopulations of dead sperm. To analyze different populations, recent studies have used single-cell analysis [38–40], flow cytometry of capacitated sperm [5, 32, 41–43], and combinations of both [44, 45]. In particular, using single-cell analysis, Arnoult et al. [14] have shown that only a fraction of the sperm undergo hyperpolarization during capacitation. These authors concluded that the measured Em of approximately −65 mV results from the combination of at least two sperm subpopulations, one with an Em of approximately −35 mV, similar to the one from noncapacitated sperm, and the other one of approximately −80 mV, closer to the theoretical K^+ equilibrium. Although single-cell analysis is excellent for detecting local and population sperm heterogeneities, this approach is not useful for high-throughput studies. On the other hand, flow cytometry can analyze tens of thousands of cells in a fraction of the time required for single-cell studies.

We have previously used Na^+ Green fluorescent probes in whole populations and a combination of CoroNa Red and propidium iodide (PI) in flow cytometry analysis to investigate how intracellular Na^+ changes during capacitation [32]. In the present work, we used anionic fluorescent voltage-sensitive probes ($DiSBAC_2(3)$) to investigate the behavior of a sperm population in regard to its Em. For this purpose, we double stained sperm suspensions with both $DiSBAC_2(3)$ and PI to analyze Em changes in live sperm. These experiments show that only a fraction of the sperm incubated under capacitating conditions undergoes hyperpolarization. Our experiments also indicate that inhibitors of either PKA or SLO3 prevent hyperpolarization, and that sperm from *Slo3* knockout (KO) mice do not display a hyperpolarized population. Overall, our observations are consistent with the hypothesis that, in a subpopulation of capacitated mouse sperm, SLO3 K^+ channels are activated downstream of a cAMP/PKA signaling pathway, causing hyperpolarization of the sperm plasma membrane.

MATERIALS AND METHODS

Materials

Chemicals were obtained from the following sources: bovine serum albumin (BSA; fatty acid-free), dibutyryl-cAMP (db-cAMP), 3-isobutyl-1-methylxanthine (IBMX), amiloride hydrochloride hydrate, carbonyl cyanide m-chlorophenylhydrazone, valinomycin, clofilium tosylate, and progesterone from Sigma; H-89 from Cayman Chemical Company; rabbit monoclonal anti-phospho-PKA substrate (clone 100G7E) from Cell Signaling (Danvers, MA); anti-phosphotyrosine (pY) monoclonal antibody (clone 4G10) from EMD Millipore; horseradish peroxidase-conjugated anti-mouse and anti-rabbit IgG from Jackson ImmunoResearch Laboratories (West Grove, PA) and GE Life Sciences, respectively; and PI, $DiSBAC_2(3)$ fluorescent voltage sensor probes, and 3,3′-dipropylthiadicarbocyanine iodide (DiSC3(5)) from Invitrogen/Life Technologies.

Mouse Sperm Preparation

CD1 retired male breeders (Charles River Laboratories, Wilmington, MA), acrosin-GFP (Acr-GFP) transgenic male (7–8 wk old), and *Slo3*$^{-/-}$ male mice (7–8 wk old) were used in accordance with Institutional Animal Care and Use Committee at the University of Massachusetts-Amherst guidelines. The Acr-GFP CF1 is a transgenic mouse line that accumulates mutated green fluorescent protein (EGFP) in the sperm acrosome [46]. Sperm were obtained from cauda epididymis in a 1-ml drop of Whitten Hepes-buffered medium. This medium does not support capacitation unless supplemented with 5 mg/ml BSA (fatty acid free) and 15–25 mM of $NaHCO_3$. After 10 min, the fraction of motile sperm was diluted four times in the appropriate medium, depending on the experiment performed. Media supplemented with BSA, but not with HCO_3^-, do not support capacitation-associated processes, such as the activation of cAMP-dependent pathways, the increase in tyrosine phosphorylation, and the ability to fertilize in vitro. Therefore, we have used this medium lacking only HCO_3^- as not supporting capacitation. For capacitation, $NaHCO_3$ was added to final concentrations of 15–25 mM. Sperm were incubated in capacitation medium at 37°C for different time periods, depending on the experimental design. To test the effect of different compounds (e.g. clofilium, amiloride, and H89), sperm were preincubated with inhibitors in noncapacitating medium for 15 min prior to beginning of the capacitating period.

SDS-PAGE and Immunoblotting

Western blots were conducted as previously described [8]. Briefly, after treatment, sperm were collected by centrifugation, washed in 1 ml of PBS, resuspended in Laemmli sample buffer without β-mercaptoethanol, and boiled for 5 min. After centrifugation, 5% β-mercaptoethanol was added to the supernatants, and the mixture was boiled again for 5 min. Protein extracts equivalent to $1–2 \times 10^6$ sperm were loaded per lane and subjected to SDS-PAGE and electrotransfer to polyvinylidene fluoride (PVDF) membranes (Bio-Rad) at 250 mA for 60 min on ice. Membranes were treated with 5% fat-free milk in Tris-buffered saline (TBS) containing 0.1% Tween 20 (T-TBS) for anti-pPKA immunodetection and with 20% fish skin gelatin (Sigma) in T-TBS for anti-pY. Antibodies were diluted in T-TBS as follows: 1/10 000 for anti-PY (clone 4G10), 1/5000 for anti-pPKA (clone 100G7E). After incubation with secondary antibodies (1/10 000 in T-TBS), enhanced chemiluminescence detection kit (ECL plus; GE Healthcare) was used according to the manufacturer's instructions. Anti-PY blots were developed by ECL (regular strength). Tyrosine-phosphorylated hexokinase, which is constitutively phosphorylated on tyrosine residues and does not change its level of phosphorylation during capacitation [47], served as a loading control. When necessary, PVDF membranes were stripped at 65°C for 15 min in 2% SDS, 0.74% β-mercaptoethanol, 62.5 mM Tris, pH 6.5, and washed six times for 5 min in T-TBS. In all experiments, molecular masses were expressed in kDa.

Sperm Analysis by Flow Cytometry

Sperm from cauda epididymis were allowed to swim in Whitten Hepes-buffered medium for 10 min. These sperm were incubated in Whitten Hepes-buffered media containing 5 mg/ml of BSA with or without the addition of 25 mM $NaHCO_3$ for a period of 60 min at 37°C. To test the effect of different compounds (e.g. clofilium, amiloride, and H-89), sperm were incubated with the respective compound for 15 min prior to incubation in capacitating medium. These sperm were then loaded with 15 μM of $DiSBAC_2(3)$ fluorescent voltage sensor by incubation for 30 min at 37°C in Whitten Hepes-buffered medium containing (or not containing) 25 mM $NaHCO_3$. Before assaying the sperm by flow cytometry, sperm suspensions were filtered through a 100-μm nylon mesh (Small Parts, Inc.) as previously described [31], and 2.1 μM of propium iodide (PI) was added. Analyses were conducted using an LSR II flow cytometer (Becton Dickinson, San Jose, CA). $DiSBAC_2(3)$, PI, and GFP were excited using a 488-nm argon excitation laser. Nonviable cells became PI positive, and their red fluorescent signal detected as fluorescence of wavelength >670 nm. Orange fluorescence from $DiSBAC_2(3)$-positive cells was detected at 561–606 nm. Finally, acrosome-intact sperm cells remained GFP positive, and their green fluorescence detected at 515–545 nm. The three indicators had minimal emission overlap. Compensation was done as per Roederer guidelines (available at http://www.drmr.com/compensation). Non-sperm events were gated out from analyses by judging the events' scatter properties, as detected in the forward-scatter (FSC) and sideways-scatter (SSC) detector, respectively (scatter-gated sperm analysis). Recording of scatter and fluorescent properties of all events stopped when 50 000 events were reached. Two-dimensional plots of SSC and FSC properties, as well as of PI fluorescence or GFP versus $DiSBAC_2(3)$ fluorescence, were obtained using FlowJo v7.6 software (Flowjo, LLC, Data Analysis Software, Ashland, OR). Average values of $DiSBAC_2(3)$ fluorescence were calculated with the equation, $(F/F0) \times 100$, where F0 corresponds to $DiSBAC_2(3)$ fluorescence from live sperm incubated for 1 h in noncapacitating conditions and F corresponds to the respective experimental condition (e.g., clofilium, amiloride, capacitating conditions, etc).

Em Assessment in Sperm Populations

Em was measured as previously described [18]. Briefly, sperm were collected as indicated above, diluted in the appropriate medium, and capacitated

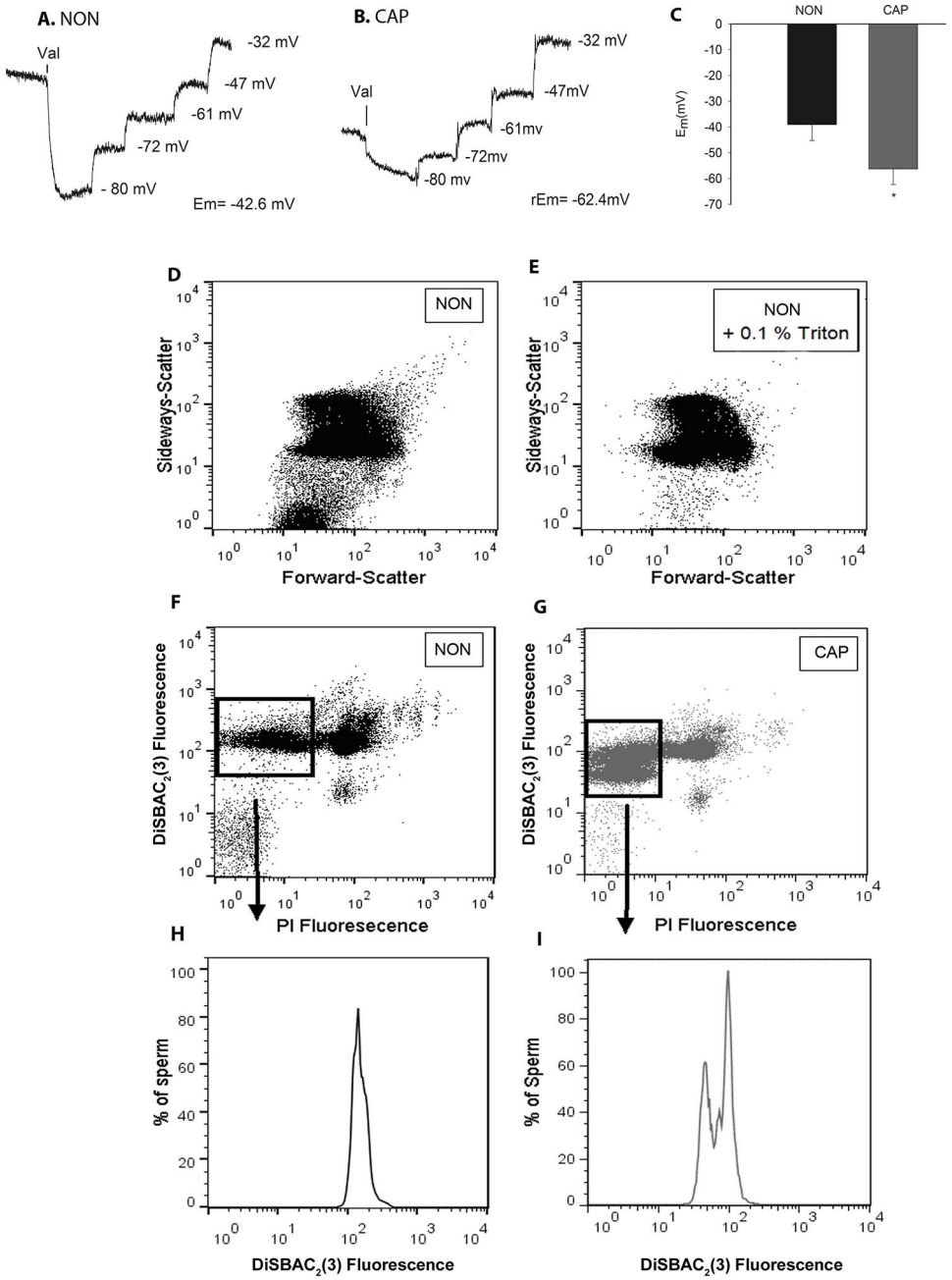

FIG. 1. Flow cytometry analysis reveals that capacitated sperm are composed of two subpopulations depicting different Ems. **A**–**C**) Whole-population analysis. Em was measured in mouse sperm in Whitten medium by using 1 μM DiSC3(5) and 1 μM carbonyl cyanide m-chlorophenylhydrazone (CCCP) to collapse mitochondrial potential. Representative fluorescence traces were used to measure resting Em, which show noncapacitated (**A**) or capacitated (**B**) sperm, and the calibration obtained by adding 1 μM valinomycin followed by sequential additions of K^+. **C**) Summary of the sperm Em under different conditions (mean ± SEM; n = 3; $*P \leq 0.05$). **D**–**I**) Flow cytometry analysis. After swimming in Whitten Hepes-buffered medium for 10 min, cauda epididymal sperm were capacitated, or not, in Whitten Hepes-buffered medium containing BSA with the addition of 15 mM HCO_3^- (CAP), or not (NON), for 1 h. Then, the sperm were loaded with 15 μM of $DiSBAC_2(3)$ fluorescent voltage sensor in Whitten Hepes-buffered medium containing $NaHCO_3$, or not, at 37°C. After 30-min incubation, PI was added and the sperm population analyzed by flow cytometry. **D** and **E**) Two-dimensional dot plot SSC versus FSC analysis of NON capacitated sperm in the absence (**D**) or in the presence (**E**) of 0.1 % triton. These analyses allowed differentiating events corresponding, or not, to sperm cells as explained in *Results*. **F** and **G**) Sperm events were selected for $DiSBAC_2(3)$ versus PI two-dimensional fluorescence dot plot analysis of sperm incubated under conditions that do not support capacitation (**F**: NON) or do support capacitation (**G**: CAP). Two-dimensional dot plots shown in **F** and **G** were used to distinguish between sperm with low (live) and high (dead) PI staining. **H** and **I**) Live sperm populations of sperm incubated under conditions that do not support (NON) or do support (CAP) capacitation were used independently for histogram analysis depicting percentage of sperm versus $DiSBAC_2(3)$ fluorescence.

for different time periods, depending on the experiment. At 8 min before the measurement, 1 μM DiSC3(5) (final concentration) was added to the sperm suspension and further incubated for 5 min at 37°C. One μM carbonyl cyanide m-chlorophenylhydrazone (final concentration) was then added to collapse mitochondrial potential, and sperm were incubated for an additional 2 min. After this period, 1.5 ml of the suspension was transferred to a gently stirred cuvette at 37°C, and the fluorescence (620/670 nm excitation/emission) was recorded continuously. Calibration was performed as described previously [23] by adding 1 μM valinomycin and sequential additions of KCl.

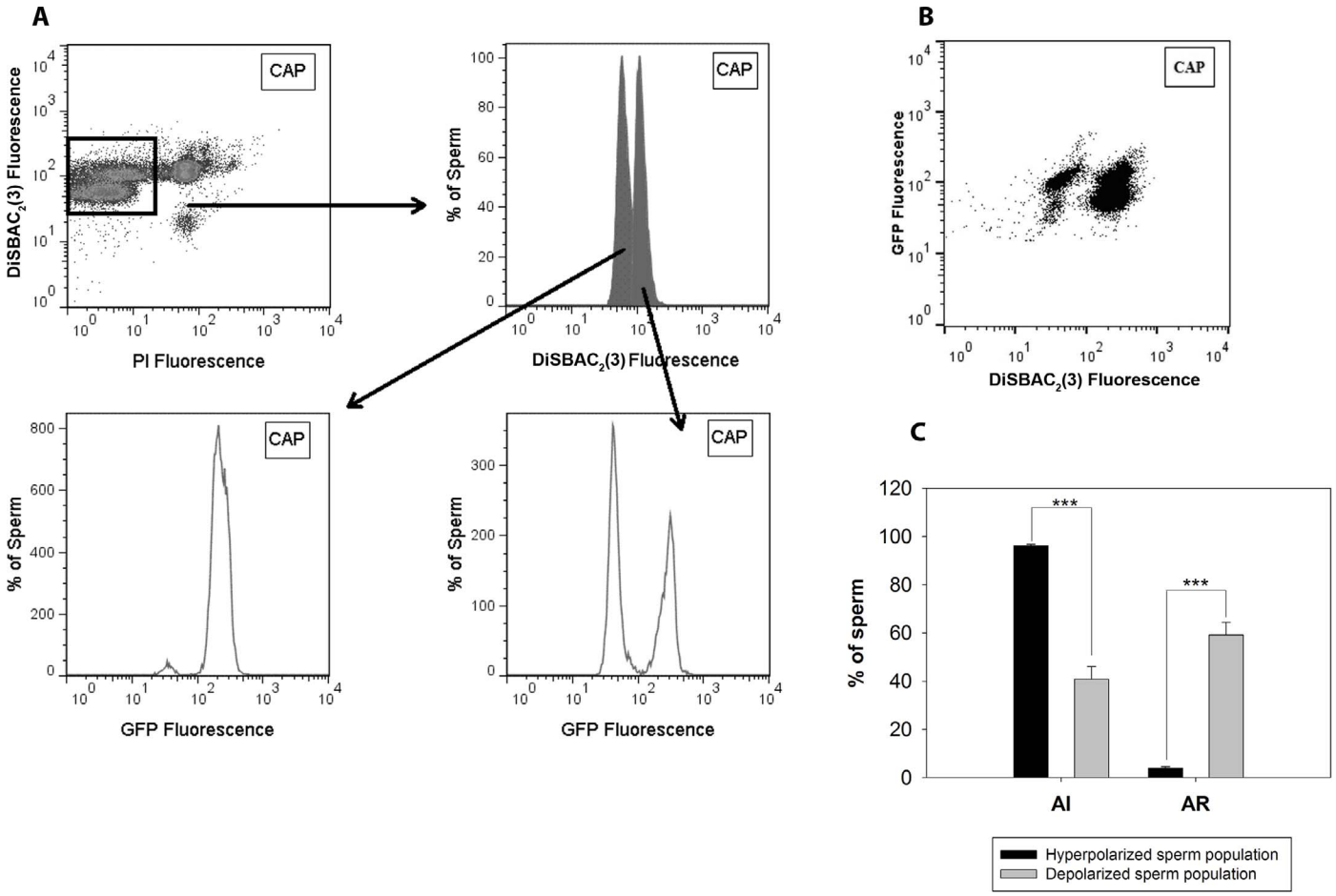

FIG. 2. Sperm belonging to the hyperpolarized capacitated subpopulation has not undergone the AR. **A**) Flow cytometry analyses of sperm containing GFP in their acrosomes. Cauda epididymal sperm containing GFP in their acrosomes were obtained from Acr-GFP CF1 mice in noncapacitating medium. These sperm were incubated in media that support capacitation and were loaded with $DiSBAC_2(3)$ for 60 min. Before flow cytometry, PI was added to the sperm suspension. Two-dimensional $DiSBAC_2(3)$ versus PI fluorescence dot plots of Acr-GFP sperm were used to analyze CAP (**A**) live and dead sperm. Live populations were then analyzed for their individual hyperpolarization states using $DiSBAC_2(3)$ fluorescence histograms. The spontaneous AR in the capacitated hyperpolarized live sperm population was further analyzed by GFP fluorescence histograms in which only one subpopulation of cells containing high GFP with intact acrosomes can be observed (lower left panel). In contrast, in the capacitated depolarized live sperm population (lower right panel), two populations of cells containing high GFP with intact acrosomes and or low GFP without acrosomes can be distinguished. **B**) Dot plot analysis of GFP-containing versus DisBac2(3) fluorescence. Results from **A** were analyzed using the GFP content versus DisBac2(3) fluorescence. **C**) Percentage of hyperpolarized versus depolarized cells in acrosome intact (AI) or AR sperm. The experiment shown in **A** and **B** was repeated seven times and the percentage of hyperpolarized versus depolarized sperm calculated in each repeat for AI or AR sperm. Data are expressed as mean percentage ± SEM; n = 7; $***P \leq 0.001$.

Fluorescence Microscopy Analysis

To verify staining patterns of GFP-positive acrosomes, sperm suspensions were fixed with 4% of paraformaldehyde and then mounted on a slide, as previously described [48]. Fluorescence images of sperm were captured with a Zeiss Axiovert 200M microscope outfitted with a ×60 oil immersion objective and a Hamamatsu Orca-AG cooled CCD camera controlled by AxioVision software 4.6 (Zeiss).

Statistics

Statistical analyses were performed using SigmaPlot (version 10; Systat Software, Inc., San Jose, CA). In order to account for sperm sample variability between males, we used a paired *t*-test. Data represent mean ± SEM. *P* values of ≤ 0.05, ≤ 0.01, or ≤ 0.001 were considered to indicate statistically significant differences.

RESULTS

Only a Sperm Subpopulation Undergoes Plasma Membrane Hyperpolarization During Capacitation

The sperm Em can be measured in whole populations using the cationic fluorescent probe, $DiSC_3(5)$. This method is based on the distribution of the positively charged fluorescent probe, which is quenched inside the cell. Measurements are achieved by calibration with the K^+ ionophore valinomycin and gradual increases in the extracellular K^+ concentration, as previously described [16]. Using these population analyses, under non-capacitating or capacitating conditions, the sperm Em was of approximately −40 mV and −60 mV, respectively (Fig. 1, A–C). To investigate how individual cells contribute to the overall Em, sperm were loaded with the anionic dye, $DiSBAC_2(3)$, along with PI to differentiate between live and dead sperm, and the distribution of their Em analyzed by flow cytometry. Contrary to $DiSC_3(5)$, the $DiSBAC_2(3)$ fluorescence increases inside the cell, and is therefore more suitable for flow

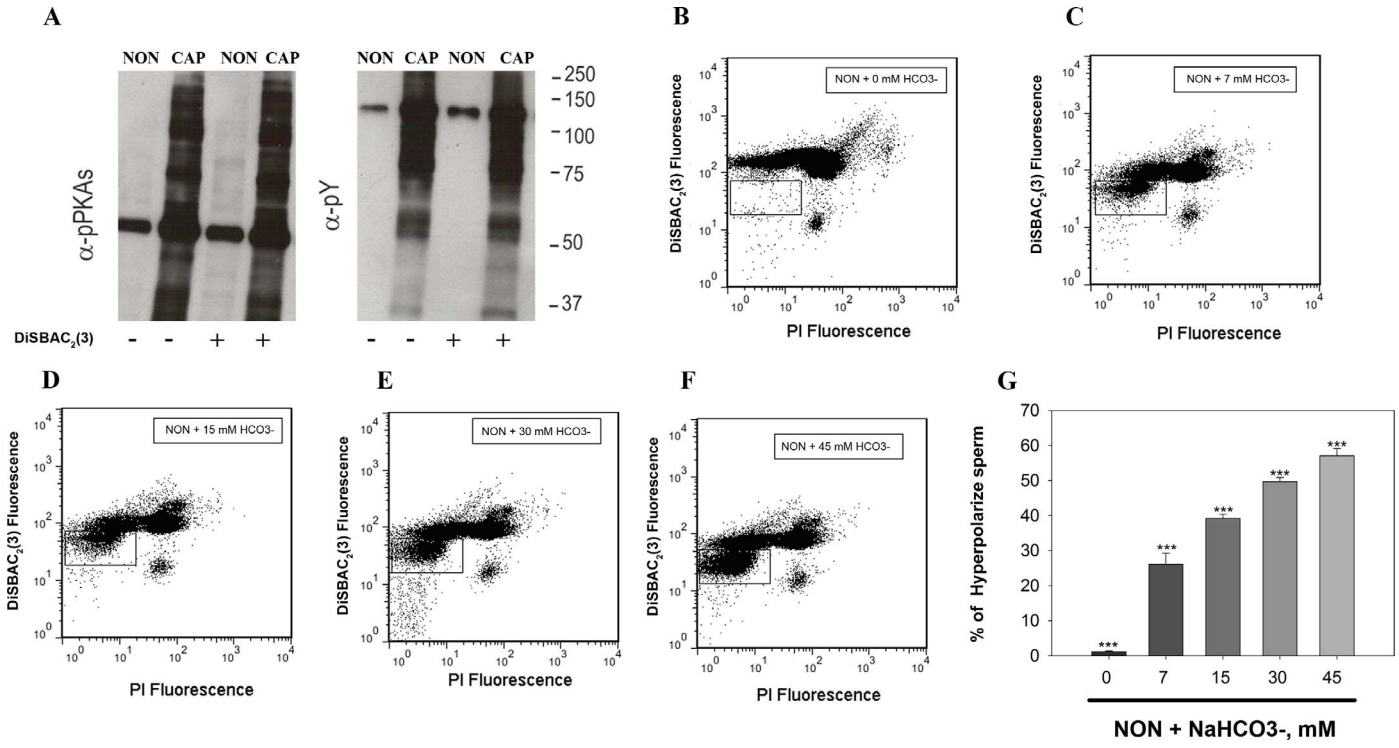

FIG. 3. The capacitation-associated hyperpolarization is dependent on the extracellular HCO_3^- concentration. Cauda epididymal sperm were capacitated in Whitten Hepes-buffered medium containing BSA and different HCO_3^- concentrations during 1 h and loaded with $DiSBAC_2(3)$, as described in the *Materials and Methods*, for 30 min. **A**) DiSBac2(3) does not affect capacitation-associated phosphorylation processes. Sperm incubated in conditions that support (CAP) or do not support (NON) capacitation for 1 h and loaded with $DiSBAC_2(3)$, or not, for 30 min were analyzed by Western blot using anti-phospho PKA substrates (α-pPKAs, left panel) or anti-phosphotyrosine antibodies (α-PY, right panel). **B**–**G**) Flow cytometry analysis of Em of sperm incubated with increasing HCO_3^- concentrations. Two-dimensional fluorescence dots plots of $DiSBAC_2(3)$ versus PI of sperm incubated with 0 (**B**), 7 (**C**), 15 (**D**), 30 (**E**), and 45 (**F**) mM of $HCO3^-$. **G**) The experiment was repeated three times and the percentage of hyperpolarized live sperm plotted versus the extracellular HCO_3^- concentration. Data represent average percentage values ± SEM; n = 3; $^{***}P \leq 0.001$.

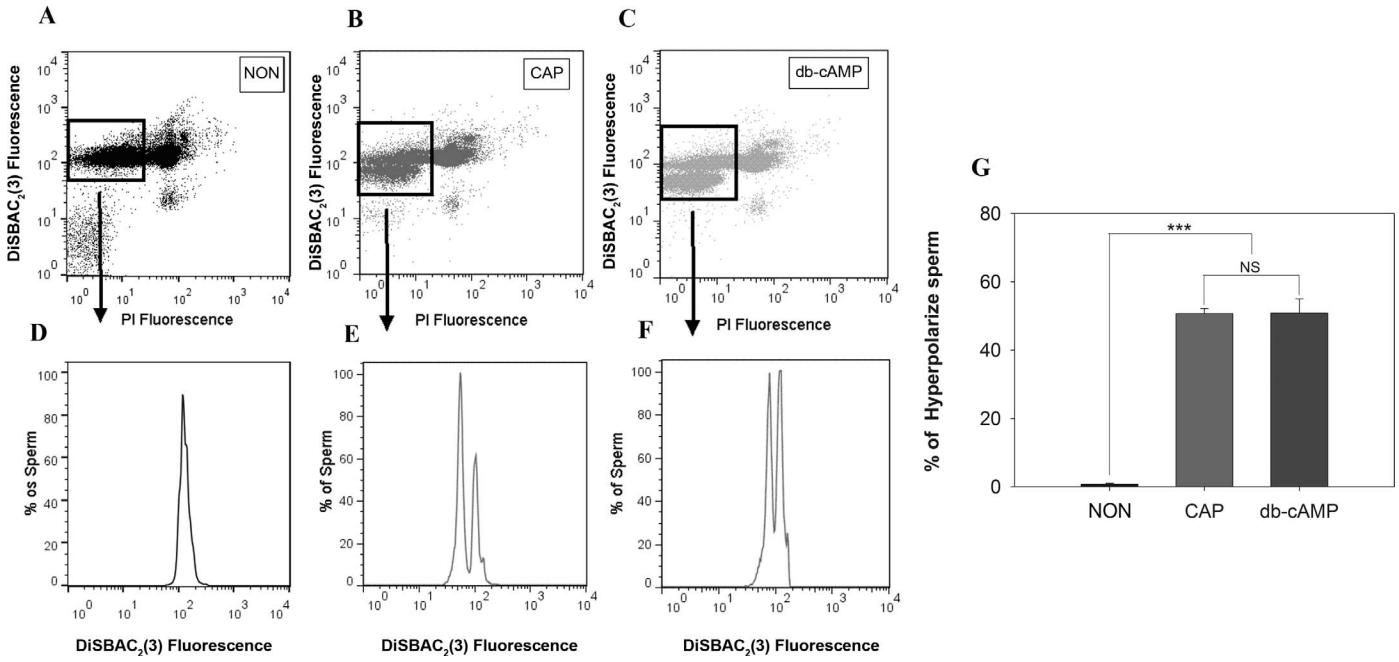

FIG. 4. cAMP agonists induced hyperpolarization in conditions that do not support capacitation. Cauda epididymal sperm were recovered in media without HCO_3^-, which does not support capacitation. Aliquots of the sperm suspension were incubated in conditions described below for an additional hour and then loaded with $DiSBAC_2(3)$, as described in the *Materials and Methods*, for 30 min. **A**–**C**) PI versus $DiSBAC_2(3)$ two-dimensional dot plots of sperm incubated in the absence of HCO_3^- (**A**, NON), in media in the presence of 24 mM HCO_3^- (**B**, CAP), or in the absence of HCO_3^- and in the presence of 1 mM db-cAMP and 100 μM IBMX (**C**, db-cAMP). The respective live populations were then analyzed for their hyperpolarization states using $DiSBAC_2(3)$ fluorescence histograms. Vertical arrows show the correspondence of the dot plots (**A**–**C**) with the histograms (**D**–**F**). Data in **G** represent mean percentage of hyperpolarized live sperm ± SEM; n = 3; $^{***}P \leq 0.001$; NS, nonsignificant) from three independent experiments.

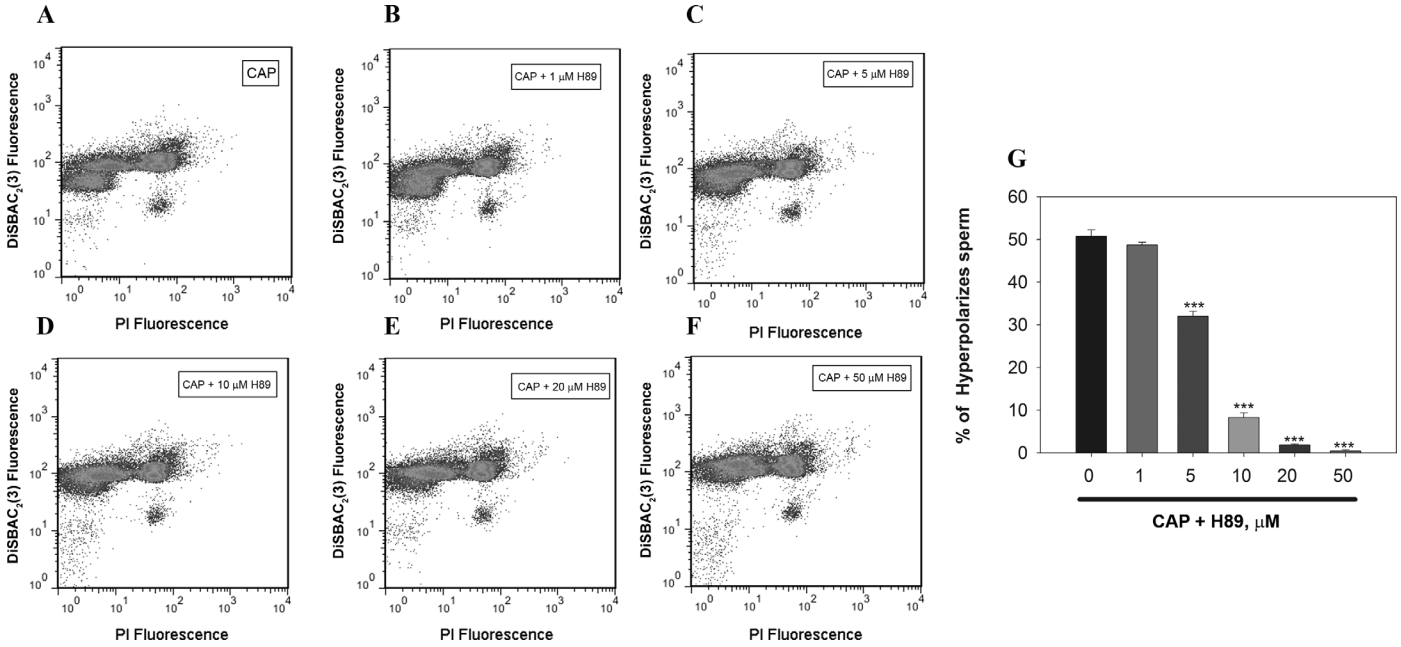

FIG. 5. PKA inhibition by H-89 blocks hyperpolarization of sperm incubated in capacitation-supporting media. Cauda epididymal sperm were incubated in media that support capacitation in the absence (**A**, CAP) or in the presence of increasing concentrations of H-89 (1, 5, 10, 20, and 50 μM; **B**–**F**, respectively) for 1 h and then loaded with $DiSBAC_2(3)$, as described in the *Materials and Methods*, for 30 min. Sperm populations were analyzed using $DiSBAC_2(3)$ versus PI two-dimensional dot plots of sperm in the aforementioned conditions. Three independent experiments were conducted and data (**G**) are presented as the mean ± SEM percentage of hyperpolarized live sperm (***$P \leq 0.001$).

cytometry analysis. Considering the $DiSBAC_2(3)$ properties, a more hyperpolarized sperm population would present less overall fluorescence due to anionic dye cell efflux. To discriminate sperm cells from nonsperm particles passing through the flow cytometer detector, two-dimensional SSC-FSC scatter dot plots were used in the absence and in the presence of 0.1% Triton X-100 (Fig. 1, D and E) as previously described [32]. Once nonsperm events were gated out, two-dimensional fluorescence dot plots of $DiSBAC_2(3)$ versus PI (to label DNA of dying cells) were created. These dot plots were used for the analysis of Em changes in sperm incubated in media that either do not support (BSA; Fig. 1F) or support (Fig. 1G) capacitation. A subpopulation of capacitated live sperm (negative for PI staining) when compared to noncapacitated live sperm exhibited a lower $DiSBAC_2(3)$ fluorescence, indicating that those cells had undergone Em hyperpolarization (Fig. 1, H and I). As expected, increasing extracellular K^+ blocked the capacitation-induced sperm Em hyperpolarization in a concentration-dependent manner, and consequently the low $DiSBAC_2(3)$ fluorescence sperm subpopulation was not detected (Supplemental Fig. S1; Supplemental Data are available online at www.biolreprod.org). Altogether, these data indicate that the average Em observed in population analyses of capacitated sperm has at least two distinct components: one arising from sperm having an Em close to that of noncapacitated cells, and another from those undergoing hyperpolarization.

Recently, we have shown that sperm hyperpolarization is necessary and sufficient for an agonist-induced AR [15]. Considering that the Em from a capacitated sperm population is typically taken as the average between two subpopulations, the status of the acrosome in these subpopulations was evaluated using genetically modified mice that carry Acr-GFP in their sperm acrosomes and lose it after the AR (Supplemental Fig. S2) [46]. Similarly to wild type, we found that capacitated GFP-containing sperm populations are composed by two different subpopulations: one with more hyperpolarized plasma membrane than the other (Fig. 2, A–C). Interestingly, this hyperpolarized subpopulation is composed almost completely of GFP-positive sperm (Fig. 2C). On the other hand, the cell subpopulation depicting a more depolarized membrane (or more positive Em) is composed of both intact and acrosome-reacted sperm (Fig. 2, A and C). Another representation of these data plotting GFP versus $DisBAC_2(3)$ fluorescence of the live-sperm population shows that AR sperm are composed almost exclusively of the depolarized population, and that almost all hyperpolarized sperm have an intact acrosome (Fig. 2C).

The Capacitation-Induced Sperm Hyperpolarization Is Mediated by Activation of a cAMP/PKA Pathway

Among ion fluxes occurring during capacitation, transport of HCO_3^- [23] constitutes one essential step in its initiation. Influx of HCO_3^- into sperm promotes cAMP synthesis through activation of the atypical soluble adenylyl cyclase 10 [49, 50] and subsequent PKA activation. This activation of a cAMP-dependent pathway is upstream of the capacitation-associated increase in tyrosine phosphorylation [51]. To investigate the role of this pathway in the regulation of sperm hyperpolarization, a series of gain-of-function and loss-of-function experiments were conducted. First, the effect of $DisBAC_2(3)$ in capacitation-induced phosphorylation pathways was evaluated by Western blots using anti-phospho PKA substrates and anti-phosphotyrosine antibodies, as described previously [8]. Neither PKA activation nor the increase in tyrosine phosphorylation was affected by the dye (Fig. 3A). Second, sperm loaded with $DiSBAC_2(3)$ were incubated in either HCO_3^--free media (which does not support capacitation) or in the same media containing increasing HCO_3^- concentrations (Fig. 3, B–F). In these conditions, the percentage of sperm undergoing membrane hyperpolarization increased as a function of HCO_3^-

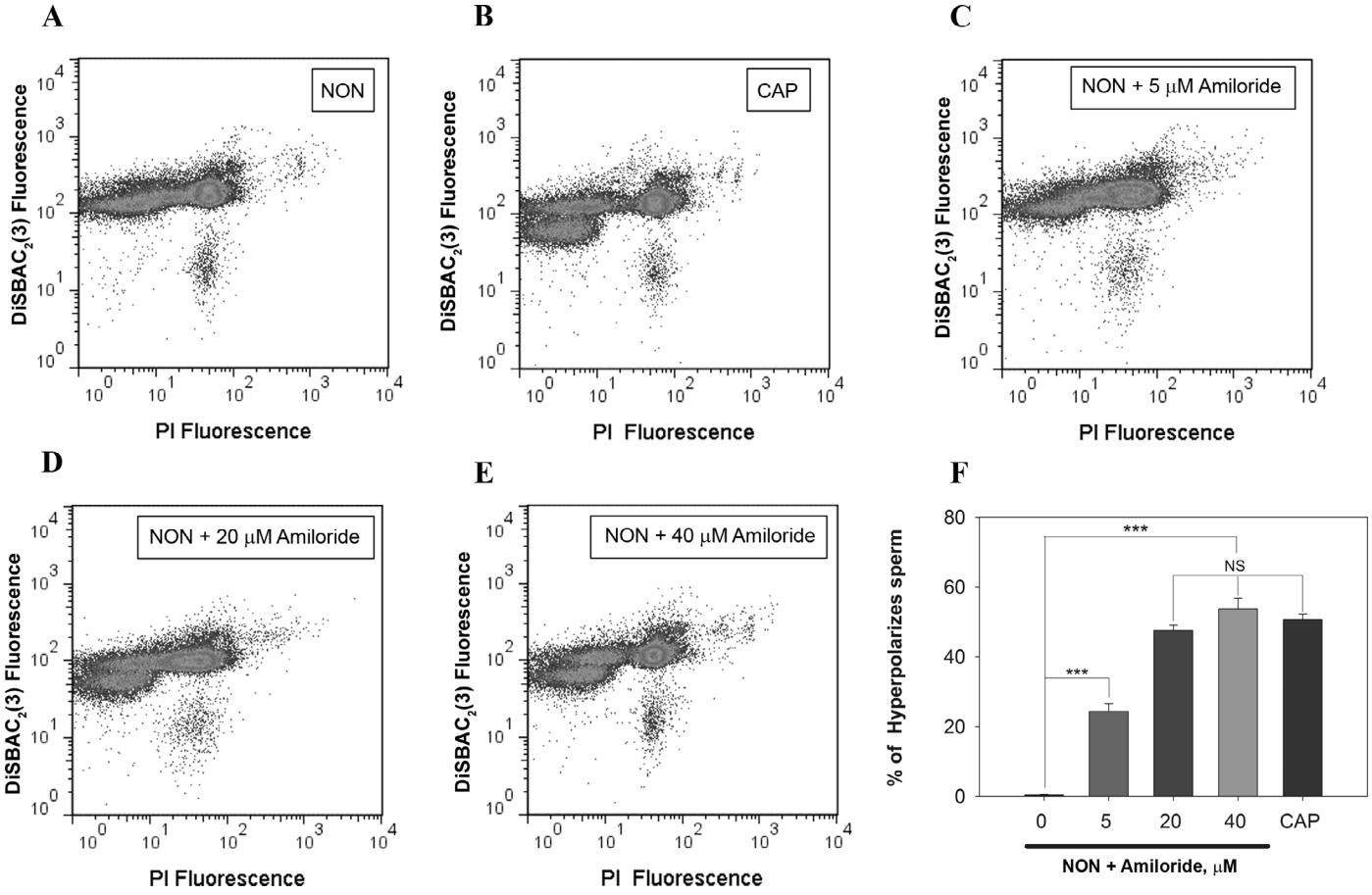

FIG. 6. Amiloride induced the sperm membrane hyperpolarization. Cauda epididymal sperm were incubated in the presence (**B**, CAP) or in the absence of HCO_3^- without (**A**, NON) or with the addition of increasing concentrations of amiloride (0, 5, 20, and 40 μM; **C**–**E**, respectively). After 1-h incubation in each condition, the sperm were loaded with $DisBAC_a(3)$, as described in the *Materials and Methods*, for 30 min and then analyzed by flow cytometry. Data are presented as $DiSBAC_2(3)$ versus PI two-dimensional dot plots. Three independent experiments were conducted, and the mean ± SEM of hyperpolarized live sperm versus amiloride concentration is presented in **F** (***$P \leq 0.001$). NS, nonsignificant.

concentration. The normalized mean fluorescence from three independent experiments was used to calculate the percentage of hyperpolarized live sperm in each condition and summarized in Figure 3G. Third, addition of cAMP agonists (1 mM db-cAMP plus 100 μM IBMX) to sperm incubated in HCO_3^--free media increased the percentage of hyperpolarized sperm to the same extent as with HCO_3^- (Fig. 4, A–F). The normalized mean fluorescence from three independent experiments was used to calculate the percentage of hyperpolarized live sperm and summarized in Figure 4G. Conversely, sperm incubation with increasing concentrations of the PKA inhibitor H89 significantly reduced the percentage of sperm membrane hyperpolarization (Fig. 5, A–G). Altogether, results shown in Figures 3–5 are consistent with the hypothesis that sperm hyperpolarization is downstream of a cAMP/PKA signaling pathway.

The Percentage of Sperm Undergoing Membrane Hyperpolarization Is Affected by Changes in Permeability to Either Na^+ or K^+ Ions

Using whole-sperm-population Em measurements, our group, as well as others [18, 21, 29, 32], has shown that conditions that either block Na^+ influx or increase K^+ efflux are able to induce sperm hyperpolarization. However, these experiments were silent regarding how different sperm subpopulations contributed to the overall Em. This problem can be addressed using flow cytometry analyses. We have previously shown that amiloride blocks an Na^+ permeability in sperm [18] and induces sperm membrane hyperpolarization in the absence of capacitation. The effect of this compound was evaluated in sperm incubated in conditions that do not support capacitation. In these conditions, amiloride increased the percentage of sperm undergoing hyperpolarization in a concentration-dependent manner (Fig. 6, A–G).

Although it is clear that Na^+ permeability plays an essential role in maintaining the resting sperm Em, recent work from our group [29] has shown that the capacitation-induced hyperpolarization may not be due to closing of Na^+ channels, but mostly to the opening of K^+ channels. Several lines of evidence suggest that, at least in mouse sperm, regulation of SLO3, a sperm-specific K^+ channel, mediates the changes in the sperm Em. To evaluate the contribution of SLO3 to the Em in sperm subpopulations, both a pharmacological and a genetic approach were used. First, in the presence of increasing concentrations of clofilium, a SLO3 inhibitor, the hyperpolarized subpopulation was not observed (Fig. 7, A–G).

Second, to further investigate the role of SLO3 channels in sperm hyperpolarization, sperm from *Slo3*$^{-/-}$ mice were loaded with $DiSCBAC_2(3)$, as described above, and incubated in conditions that support capacitation (Fig. 8, A–F). Sperm from *Slo3*-null mice were unable to exhibit a hyperpolarized sperm subpopulation during capacitation when compared to control sperm. Most interestingly, both the phosphorylation of PKA

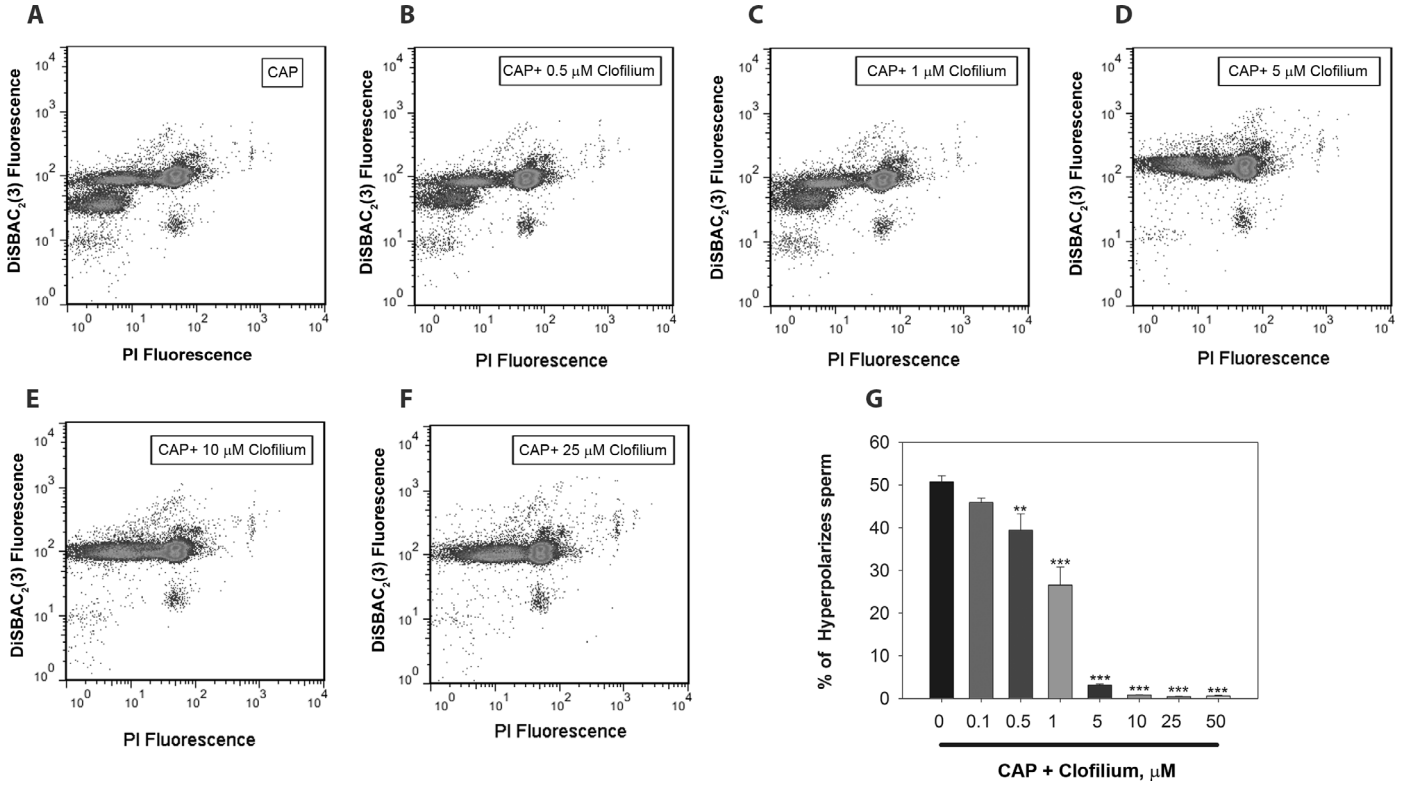

FIG. 7. Clofilium, a SLO3 channel antagonist, blocked membrane hyperpolarization of sperm incubated in conditions that support capacitation. Cauda epididymal sperm were incubated in media that support capacitation in the absence (**A**, CAP) or in the presence of increasing concentrations of Clofilium (0.1, 0.5, 1, 5, 10, 25, and 50 μM; **B**–**F**, respectively). After 1 h, sperm were loaded with DiSBAC$_2$(3) for 30 min, as described in the *Materials and Methods*. Data are presented as DiSBAC$_2$(3) versus PI two-dimensional dot plots. Data from four independent experiments are presented in **G** as mean ± SEM percentage of hyperpolarized live sperm (**$P \leq 0.01$ and ***$P \leq 0.001$).

substrates, as well as that in tyrosine residues, was not affected by clofilium in sperm from either CD1 (Fig. 8G) or *Slo3* KO (Fig. 8H) mice. These data, together with those presented above (Fig. 7), are consistent with the hypothesis that PKA activation is upstream of the changes in Em observed during sperm capacitation.

DISCUSSION

Mammalian sperm undergo capacitation in the female reproductive tract before acquiring fertilizing capacity. Studies on the capacitation process in vitro have revealed that sperm are not represented by a homogeneous population. First, in many species, computer-assisted sperm analysis has shown that not more than 20 % of the sperm population achieved hyperactivation upon capacitation [52, 53]. Second, depending on the species, between 10% and 30% of the sperm undergoes a spontaneous AR, and that, from the remaining sperm, not more than 40% can undergo the AR after being exposed to either progesterone or solubilized zona pellucidae. More surprising is the observation that, even under conditions in which $[Ca^{2+}]_i$ is artificially elevated by incubation with Ca^{2+} ionophores, such as ionomycin or A23187, only 50%–70% of sperm undergoes exocytosis. The reason for this heterogeneity is not understood. However, because, in addition to capacitation, mammalian sperm are also required to mature in the male epididymis, one possibility is that the heterogeneity is due to different stages of epididymal maturation. It can also be hypothesized that having sperm at different stages of capacitation could extend the time period in which sperm are able to fertilize, spreading in this way the reproductive fitness of the species even if a high percentage of them fails to capacitate.

In whole-population analyses, it has been well established that sperm incubated in a capacitation-supporting medium undergo: 1) an HCO_3^--dependent increase in cAMP levels followed by a rapid activation of PKA; 2) pH_i alkalinization; 3) elevation of $[Ca^{2+}]_i$; 4) hyperpolarization of the plasma membrane (Em); and 5) increase in tyrosine phosphorylation. It is not known, however, how these signaling events are activated in different fractions of the sperm population and whether the sperm undergoing one of these events (e.g. PKA activation) are the same ones experiencing the other capacitation-dependent signaling pathways. To investigate the molecular basis of sperm population heterogeneity, it is therefore necessary to find methods that can classify and separate sperm subpopulations depending on their state of capacitation. Among these methodologies, single cell analysis allows to classification of a particular cell into different stages of capacitation [38–40]. We have previously used Fluo-4 to evaluate the number of sperm depicting increases in $[Ca^{2+}]_i$ after treatment with solubilized zona pellucidae, and where they may occur [15]. Although these methods are very powerful, the amount of cells studied is limited. Another strategy generally used to evaluate single cell behavior in a much larger population is flow cytometry. Flow cytometry can be used to analyze different parameters in thousands of individual sperm within seconds [5, 32, 41–43]. These methods have been applied to study sperm viability, changes in mitochondrial Em, sperm size [41], and for sexing mammalian sperm using DNA staining dyes [54].

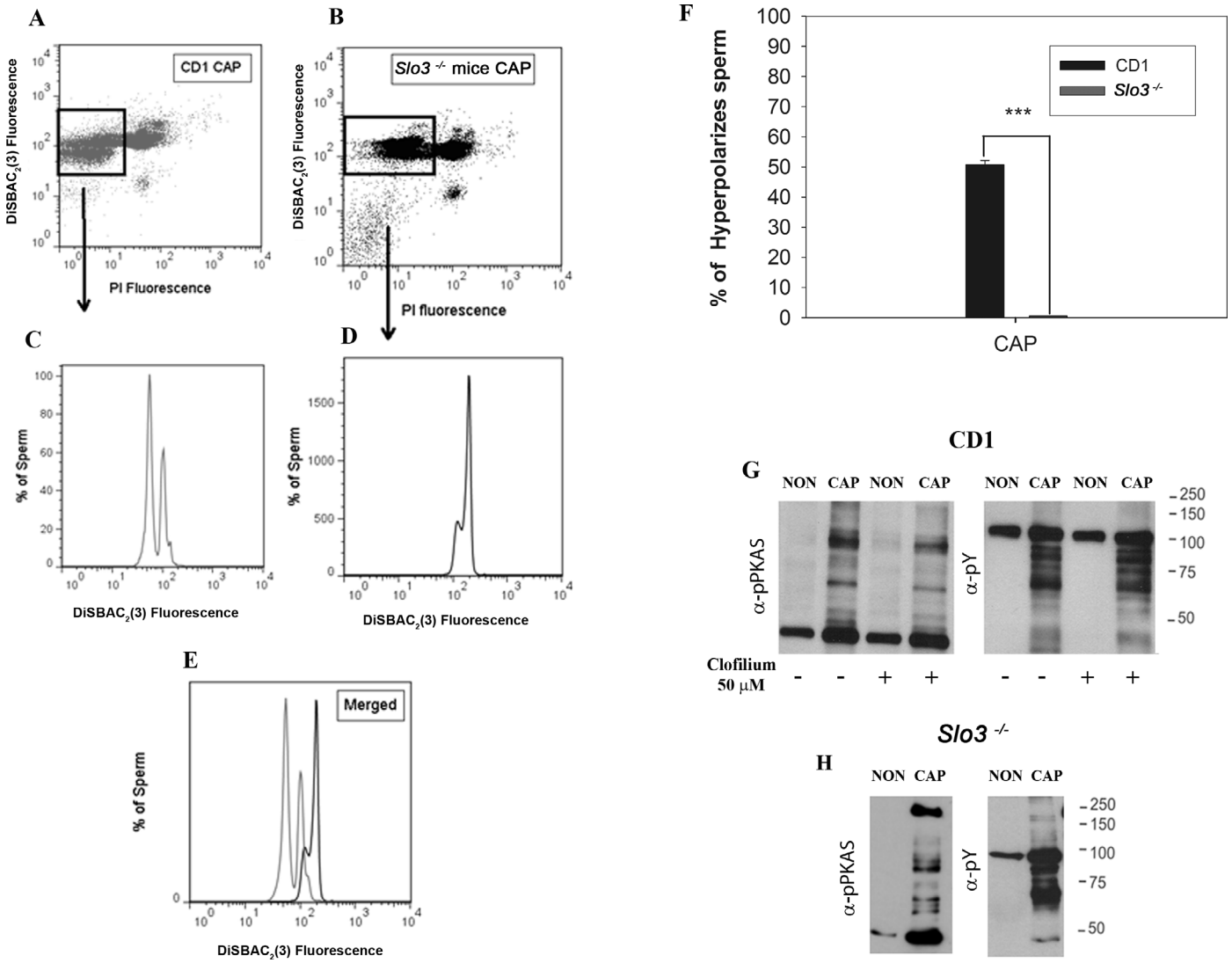

FIG. 8. Sperm from *Slo3*$^{-/-}$ mice do not undergo capacitation-associated hyperpolarization. Cauda epididymal sperm from control (**A**) and *Slo3*$^{-/-}$ (**B**) mice were incubated for 1 h in conditions that support capacitation and loaded with DiSBAC$_2$(3), as described in the *Materials and Methods*, for 30 min. The capacitation-associated hyperpolarization was analyzed using DiSBAC$_2$(3) versus PI two-dimensional fluorescence dots plots. Live sperm populations of sperm incubated under conditions that support capacitation from control and *Slo3*$^{-/-}$ mice were used for histogram analysis depicting percentage of sperm versus DiSBAC$_2$(3) fluorescence (**C** and **D**, respectively). Merged data are presented in **E**. Three independent experiments were conducted, and the mean ± SEM of hyperpolarized live sperm are presented (**F**) (***$P \leq 0.001$). **G** and **H**) Western blots using anti-p-PKAS or anti-PY antibodies of sperm extracts from control mice (**G**) and Slo3$^{-/-}$ mice (**H**) incubated in conditions that support (CAP) or do not support (NON) capacitation in the presence or absence of 50 μM of clofilium, as indicated in the figure text.

Previously, we have used flow cytometry of CoRoNa Red-loaded sperm to study how intracellular Na^+ changes during capacitation. Our results indicate that during capacitation, $[Na^+]_i$ decreases in a sperm subpopulation [32]. In the present work, we used the anionic dye DiSBAC$_2$(3) to investigate the resting Em in sperm populations incubated under different conditions. First, our results indicate that, regarding their Ems, sperm incubated in media that do not support capacitation are constituted by mainly one population. On the other hand, sperm incubated under capacitating conditions distribute in two defined subpopulations: one with similar DiSBAC$_2$(3) average fluorescence to the noncapacitated sperm single population, the other one depicting less fluorescence. These results are consistent with those measuring Em in single cells using di8-ANEPPS, a fast, voltage-sensitive fluorescent dye [14], and suggest that about 50% of capacitated sperm undergo hyperpolarization as part of the capacitation process. Second, the hyperpolarized population is almost exclusively formed by sperm presenting an intact acrosome. Third, we show here that the separation of the capacitated sperm population into two distinct subpopulations, one more hyperpolarized than the other, is downstream of a cAMP-dependent signaling pathway. This conclusion is based on findings that the percentage of hyperpolarized sperm: 1) is dependent on extracellular HCO_3^- concentration; 2) increased with the addition of permeable cAMP agonists; and 3) was inhibited by the PKA antagonist H89 in a concentration-dependent manner. Fourth, consistent with previous reports, amiloride's blockade of Na^+ permeability in sperm incubated under noncapacitating conditions increased the percentage of hyperpolarized sperm to the same level as that obtained with sperm incubated under capacitating conditions. Finally, a K^+ channel inhibitor blocked the capacitation-induced hyperpolarization, and the hyperpolarized

sperm subpopulation was not observed in sperm from *Slo3*-null mice.

As mentioned in the *Introduction*, the presence of T-type voltage-dependent CaV3 Ca^{2+} channels has been questioned [28]. However, more recently, Cohen et al. [55] have presented evidence that CaV2.3 channels participate in the regulation of the AR. These authors proposed that activation of CaV2.3 requires hyperpolarization-induced relief from voltage-dependent inactivation. More interestingly, the authors found that ~50% of the capacitated sperm population responded to the ganglioside GM1 during AR stimulation. Interestingly, we have recently presented evidence that hyperpolarization is also involved in the regulation of Ca^{2+} entry through CatSper channels [56]. Although the role of CaV channels needs to be further investigated, it has been shown that sperm incubated in conditions that block hyperpolarization fail to undergo the ZP-induced AR [20, 22, 31]. Regarding the molecular mechanisms involved in the regulation of the capacitation-induced hyperpolarization, work from several laboratories, including ours, has proposed the involvement of ENaC, CFTR, and K^+ channels in sperm hyperpolarization [57]. Sperm hyperpolarization can be explained by either a block of Na^+ channels (e.g., ENaC) and/or by activation of K^+ channels (e.g., SLO3). Our results are silent regarding these alternative hypotheses. However, in a recent work from our group using *Slo3* KO sperm [29], we presented evidence suggesting that the capacitation-induced hyperpolarization is mainly due to pH_i-regulated opening of K^+ channels, and not to closing of Na^+ channels. The SLO3 K^+ channel is a member of the high-conductance SLO K^+ channel family, and was cloned in 1998 by the Salkoff laboratory [58]. These channels are only present in mammalian sperm and are activated by intracellular alkalization and membrane depolarization [28, 32, 33]. SLO3 channels are fairly resistant to blockage by external TEA (a typical K^+ channel blocker), but are very sensitive to low concentrations of external Ba^{2+}, clofilium, and quinidine [30, 31].

The conclusion that SLO3 K^+ channels are principally responsible for the capacitation-associated hyperpolarization is based on the following previous observations [27]: 1) eliminating the contribution of the SLO3 channel, either by the use of the *Slo3* KO mutant or by pharmacological agents that block SLO3 K^+ permeability in wild-type sperm, significantly inhibits the capacitation-associated hyperpolarization of the sperm plasma membrane; 2) all experiments revealed that the increase in SLO3 K^+ permeability was the essential factor in capacitation, while a significant reduction in Na^+ permeability was not observed; and 3) an additional finding was that exposure to external pH 8 both before and after capacitation evokes membrane hyperpolarization in wild-type sperm, but not in *Slo3* KO mutant sperm. Similar results were observed in wild-type sperm incubated in the presence of pharmacological agents that block SLO3 K^+ permeability. In these experiments, a significant reduction in Na^+ permeability was not detected. Notably, these latter results suggest a role of pH_i in the regulation of the sperm Em.

Considering the necessity of PKA activation for the observed hyperpolarization, these results are consistent with the hypothesis that changes in pH_i mediate at least in part the cAMP response. In addition to the mouse, the capacitation-induced hyperpolarization has been described in stallion [59] and human [60] sperm. Altogether, findings in this article contribute to the understanding of how signaling processes involved in sperm capacitation are regulated. In addition, the experimental design employed throughout this article open new avenues of investigation to study the behavior of different sperm populations using flow cytometry and cell sorting.

ACKNOWLEDGMENT

We would like to thank Dr. Ana Maria Salicioni for her help with the Acr-GFP mouse genotyping and for critical reading of the manuscript, and Dr. Eva Wertheimer and Dr. Dario Krapf for their helpful advice.

REFERENCES

1. Yanagimachi R. Fertility of mammalian spermatozoa: its development and relativity. Zygote 1994; 2:371–372.
2. Trevino CL, Serrano CJ, Beltran C, Felix R, Darszon A. Identification of mouse trp homologs and lipid rafts from spermatogenic cells and sperm. FEBS Lett 2001; 509:119–125.
3. Visconti PE, Galantino-Homer H, Ning X, Moore GD, Valenzuela JP, Jorgez CJ, Alvarez JG, Kopf GS. Cholesterol efflux-mediated signal transduction in mammalian sperm. beta-cyclodextrins initiate transmembrane signaling leading to an increase in protein tyrosine phosphorylation and capacitation.J Biol Chem 1999; 274:3235–3242.
4. Visconti PE, Ning X, Fornes MW, Alvarez JG, Stein P, Connors SA, Kopf GS. Cholesterol efflux-mediated signal transduction in mammalian sperm: cholesterol release signals an increase in protein tyrosine phosphorylation during mouse sperm capacitation. Dev Biol 1999; 214:429–443.
5. Nakanishi T, Ikawa M, Yamada S, Toshimori K, Okabe M. Alkalinization of acrosome measured by GFP as a pH indicator and its relation to sperm capacitation. Dev Biol 2001; 237:222–231.
6. Darszon A, Guerrero A, Galindo BE, Nishigaki T, Wood CD. Sperm-activating peptides in the regulation of ion fluxes, signal transduction and motility. Int J Dev Biol 2008; 52:595–606.
7. Arcelay E, Salicioni AM, Wertheimer E, Visconti PE. Identification of proteins undergoing tyrosine phosphorylation during mouse sperm capacitation. Int J Dev Biol 2008; 52:463–472.
8. Krapf D, Arcelay E, Wertheimer EV, Sanjay A, Pilder SH, Salicioni AM, Visconti PE. Inhibition of Ser/Thr phosphatases induces capacitation-associated signaling in the presence of Src kinase inhibitors. J Biol Chem 2010; 285:7977–7985.
9. Visconti PE, Bailey JL, Moore GD, Pan D, Olds-Clarke P, Kopf GS. Capacitation of mouse spermatozoa. I. Correlation between the capacitation state and protein tyrosine phosphorylation.Development 1995; 121: 1129–1137.
10. Visconti PE, Moore GD, Bailey JL, Leclerc P, Connors SA, Pan D, Olds-Clarke P, Kopf GS. Capacitation of mouse spermatozoa. II. Protein tyrosine phosphorylation and capacitation are regulated by a cAMP-dependent pathway.Development 1995; 121:1139–1150.
11. Escoffier J, Jemel I, Tanemoto A, Taketomi Y, Payre C, Coatrieux C, Sato H, Yamamoto K, Masuda S, Pernet-Gallay K, Pierre V, Hara S, et al. Group X phospholipase A2 is released during sperm acrosome reaction and controls fertility outcome in mice. J Clin Invest 2010; 120:1415–1428.
12. Tomes CN. Molecular mechanisms of membrane fusion during acrosomal exocytosis. Soc Reprod Fertil Suppl 2007; 65:275–291.
13. Buffone MG, Foster JA, Gerton GL. The role of the acrosomal matrix in fertilization. Int J Dev Biol 2008; 52:511–522.
14. Arnoult C, Kazam IG, Visconti PE, Kopf GS, Villaz M, Florman HM. Control of the low voltage-activated calcium channel of mouse sperm by egg ZP3 and by membrane hyperpolarization during capacitation. Proc Natl Acad Sci U S A 1999; 96:6757–6762.
15. De La Vega-Beltran JL, Sanchez-Cardenas C, Krapf D, Hernandez-Gonzalez EO, Wertheimer E, Trevino CL, Visconti PE, Darszon A. Mouse sperm membrane potential hyperpolarization is necessary and sufficient to prepare sperm for the acrosome reaction. J Biol Chem 2012; 287: 44384–44393.
16. de la Sancha CU, Martinez-Cadena G, Lopez-Godinez J, Castellano LE, Nishigaki T, Darszon A, Garcia-Soto J. Rho-kinase (ROCK) in sea urchin sperm: its role in regulating the intracellular pH during the acrosome reaction. Biochem Biophys Res Commun 2007; 364:470–475.
17. Espinosa F, Darszon A. Mouse sperm membrane potential: changes induced by Ca^{2+}. FEBS Lett 1995; 372:119–125.
18. Hernandez-Gonzalez EO, Sosnik J, Edwards J, Acevedo JJ, Mendoza-Lujambio I, Lopez-Gonzalez I, Demarco I, Wertheimer E, Darszon A, Visconti PE. Sodium and epithelial sodium channels participate in the regulation of the capacitation-associated hyperpolarization in mouse sperm. J Biol Chem 2006; 281:5623–5633.
19. McPartlin LA, Visconti PE, Bedford-Guaus SJ. Guanine-nucleotide exchange factors (RAPGEF3/RAPGEF4) induce sperm membrane

depolarization and acrosomal exocytosis in capacitated stallion sperm. Biol Reprod 2011; 85:179–188.
20. Munoz-Garay C, De La Vega-Beltran JL, Delgado R, Labarca P, Felix R, Darszon A. Inwardly rectifying K(+) channels in spermatogenic cells: functional expression and implication in sperm capacitation. Dev Biol 2001; 234:261–274.
21. Santi CM, Martinez-Lopez P, de la Vega-Beltran JL, Butler A, Alisio A, Darszon A, Salkoff L. The SLO3 sperm-specific potassium channel plays a vital role in male fertility. FEBS Lett 2010; 584:1041–1046.
22. Nasu T, Fukuda Y, Hashino J, Nagahira K, Kawashima H, Noguchi C, Oikawa S, Nakanishi T. Epitope mapping of monoclonal antibodies against N-domain of carcinoembryonic antigen. Immunol Lett 1999; 67: 57–62.
23. Demarco IA, Espinosa F, Edwards J, Sosnik J, De La Vega-Beltran JL, Hockensmith JW, Kopf GS, Darszon A, Visconti PE. Involvement of a Na^+/HCO_3^- cotransporter in mouse sperm capacitation. J Biol Chem 2003; 278:7001–7009.
24. Arnoult C, Zeng Y, Florman HM. ZP3-dependent activation of sperm cation channels regulates acrosomal secretion during mammalian fertilization. J Cell Biol 1996; 134:637–645.
25. Zeng Y, Clark EN, Florman HM. Sperm membrane potential: hyperpolarization during capacitation regulates zona pellucida-dependent acrosomal secretion. Dev Biol 1995; 171:554–563.
26. Lievano A, Santi CM, Serrano CJ, Trevino CL, Bellve AR, Hernandez-Cruz A, Darszon A. T-type Ca^{2+} channels and alpha1E expression in spermatogenic cells, and their possible relevance to the sperm acrosome reaction. FEBS Lett 1996; 388:150–154.
27. Balderas E, Ateaga-Tlecuitl R, Rivera M, Gomora JC, Darszon A. Niflumic acid blocks native and recombinant T-type channels. J Cell Physiol 2012; 227:2542–2555.
28. Lishko PV, Kirichok Y, Ren D, Navarro B, Chung JJ, Clapham DE. The control of male fertility by spermatozoan ion channels. Annu Rev Physiol 2012; 74:453–475.
29. Chavez JC, de la Vega-Beltran JL, Escoffier J, Visconti PE, Trevino CL, Darszon A, Salkoff L, Santi CM. Ion permeabilities in mouse sperm reveal an external trigger for SLO3-dependent hyperpolarization. PLoS One 2013; 8:e60578.
30. Zeng XH, Yang C, Kim ST, Lingle CJ, Xia XM. Deletion of the Slo3 gene abolishes alkalization-activated K^+ current in mouse spermatozoa. Proc Natl Acad Sci U S A 2011; 108:5879–5884.
31. Acevedo JJ, Mendoza-Lujambio I, de la Vega-Beltran JL, Trevino CL, Felix R, Darszon A. KATP channels in mouse spermatogenic cells and sperm, and their role in capacitation. Dev Biol 2006; 289:395–405.
32. Escoffier J, Krapf D, Navarrete F, Darszon A, Visconti PE. Flow cytometry analysis reveals a decrease in intracellular sodium during sperm capacitation. J Cell Sci 2012; 125:473–485.
33. Hernandez-Gonzalez EO, Trevino CL, Castellano LE, de la Vega-Beltran JL, Ocampo AY, Wertheimer E, Visconti PE, Darszon A. Involvement of cystic fibrosis transmembrane conductance regulator in mouse sperm capacitation. J Biol Chem 2007; 282:24397–24406.
34. Figueiras-Fierro D, Acevedo JJ, Martinez-Lopez P, Escoffier J, Sepulveda FV, Balderas E, Orta G, Visconti PE, Darszon A. Electrophysiological evidence for the presence of cystic fibrosis transmembrane conductance regulator (CFTR) in mouse sperm. J Cell Physiol 2013; 228:590–601.
35. Xu WM, Shi QX, Chen WY, Zhou CX, Ni Y, Rowlands DK, Yi Liu G, Zhu H, Ma ZG, XF, Wang, ZH, Chen, Zhou SC, et al. Cystic fibrosis transmembrane conductance regulator is vital to sperm fertilizing capacity and male fertility. Proc Natl Acad Sci U S A 2007; 104:9816–9821.
36. Lishko PV, Kirichok Y, Ren D, Navarro B, Chung JJ, Clapham DE. The control of male fertility by spermatozoan ion channels. Annu Rev Physiol 2012; 74:453–475.
37. Escoffier J, Krapf D, Navarrete F, Darszon A, Visconti PE. Flow cytometry analysis reveals a decrease in intracellular sodium during sperm capacitation. J Cell Sci 2012; 125:473–485.
38. Arnoult C, Kazam IG, Visconti PE, Kopf GS, Villaz M, Florman HM. Control of the low voltage-activated calcium channel of mouse sperm by egg ZP3 and by membrane hyperpolarization during capacitation. Proc Natl Acad Sci U S A 1999; 96:6757–6762.
39. Escoffier J, Boisseau S, Serres C, Chen CC, Kim D, Stamboulian S, Shin HS, Campbell KP, De Waard M, Arnoult C. Expression, localization and functions in acrosome reaction and sperm motility of Ca(V)3.1 and Ca(V)3.2 channels in sperm cells: an evaluation from Ca(V)3.1 and Ca(V)3.2 deficient mice. J Cell Physiol 2007; 212:753–763.
40. Fukami K, Yoshida M, Inoue T, Kurokawa M, Fissore RA, Yoshida N, Mikoshiba K, Takenawa T. Phospholipase Cdelta4 is required for Ca^{2+} mobilization essential for acrosome reaction in sperm. J. Cell Biol 2003; 161:79–88.
41. Martinez-Pastor F, Mata-Campuzano M, Alvarez-Rodriguez M, Alvarez M, Anel L, de Paz P. Probes and techniques for sperm evaluation by flow cytometry. Reprod Domest Anim 2010; 45(Suppl 2):67–78.
42. Piehler E, Petrunkina AM, Ekhlasi-Hundrieser M, Topfer-Petersen E. Dynamic quantification of the tyrosine phosphorylation of the sperm surface proteins during capacitation. Cytometry A 2006; 69:1062–1070.
43. Tao J, Critser ES, Critser JK. Evaluation of mouse sperm acrosomal status and viability by flow cytometry. Mol Reprod Dev 1993; 36:183–194.
44. De Blas GA, Darszon A, Ocampo AY, Serrano CJ, Castellano LE, Hernandez-Gonzalez EO, Chirinos M, Larrea F, Beltran C, Trevino CL. TRPM8, a versatile channel in human sperm. PLoS One 2009; 4:e6095.
45. Flesch FM, Brouwers JF, Nievelstein PF, Verkleij AJ, van Golde LM, Colenbrander B, Gadella BM. Bicarbonate stimulated phospholipid scrambling induces cholesterol redistribution and enables cholesterol depletion in the sperm plasma membrane. J Cell Sci 2001; 114: 3543–3555.
46. Nakanishi T, Ikawa M, Yamada S, Parvinen M, Baba T, Nishimune Y, Okabe M. Real-time observation of acrosomal dispersal from mouse sperm using GFP as a marker protein. FEBS Lett 1999; 449:277–283.
47. Porambo JR, Salicioni AM, Visconti PE, Platt MD. Sperm phosphoproteomics: historical perspectives and current methodologies. Expert Rev Proteomics 2012; 9:533–548.
48. Escoffier J, Couvet M, de Pomyers H, Ray PF, Seve M, Lambeau G, De Waard M, Arnoult C. Snake venoms as a source of compounds modulating sperm physiology: Secreted phospholipases A2 from *Oxyuranus scutellatus scutellatus* impact sperm motility, acrosome reaction and in vitro fertilization in mice. Biochimie 2010; 92:826–836.
49. Esposito G, Jaiswal BS, Xie F, Krajnc-Franken MA, Robben TJ, Strik AM, Kuil C, Philipsen RL, van Duin M, Conti M, Gossen JA. Mice deficient for soluble adenylyl cyclase are infertile because of a severe sperm-motility defect. Proc Natl Acad Sci U S A 2004; 101:2993–2998.
50. Hess KC, Jones BH, Marquez B, Chen Y, Ord TS, Kamenetsky M, Miyamoto C, Zippin JH, Kopf GS, Suarez SS, Levin LR, Williams CJ, et al. The ''soluble'' adenylyl cyclase in sperm mediates multiple signaling events required for fertilization. Dev Cell 2005; 9:249–259.
51. Visconti PE. Understanding the molecular basis of sperm capacitation through kinase design. Proc Natl Acad Sci U S A 2009; 106:667–668.
52. Goodson SG, Zhang Z, Tsuruta JK, Wang W, O'Brien DA. Classification of mouse sperm motility patterns using an automated multiclass support vector machines model. Biol Reprod 2011; 84:1207–1215.
53. Mortimer ST. CASA—practical aspects. J Androl 2000; 21:515–524.
54. Johnson LA. Sexing mammalian sperm for production of offspring: the state-of-the-art. Anim Reprod Sci 2000; 60–61:93–107.
55. Cohen R, Buttke DE, Asano A, Mukai C, Nelson JL, Ren D, Miller RJ, Cohen-Kutner M, Atlas D, Travis AJ. Lipid modulation of calcium flux through CaV2.3 regulates acrosome exocytosis and fertilization. Dev Cell 2014; 28:310–321.
56. Chavez JC, Ferreira Gregorio J, Butler A, Trevino CL, Darszon A, Salkoff L, Santi CM. SLO3 K^+ channels control calcium entry through CATSPER channels in sperm. J Biol Chem 2014; 289:32266–32275.
57. Visconti PE, Krapf D, de la Vega-Beltran JL, Acevedo JJ, Darszon A. Ion channels, phosphorylation and mammalian sperm capacitation. Asian J Androl 2011; 13:395–405.
58. Schreiber M, Wei A, Yuan A, Gaut J, Saito M, Salkoff L. Slo3, a novel pH-sensitive K^+ channel from mammalian spermatocytes. J Biol Chem 1998; 273:3509–3516.
59. Bedford SJ, Gowdy HL, Hinrichs K. Comparison of the longevity of motility of stallion spermatozoa incubated at 38 degrees C in different capacitating media and containers. Theriogenology 1999; 51:637–646.
60. Trevino CL, Felix R, Castellano LE, Gutierrez C, Rodriguez D, Pacheco J, Lopez-Gonzalez I, Gomora JC, Tsutsumi V, Hernandez-Cruz A, Fiordelisio T, Scaling AL, et al. Expression and differential cell distribution of low-threshold Ca(2+) channels in mammalian male germ cells and sperm. FEBS Lett 2004; 563:87–92.